NMR Solution Structure of Neurotensin in Membrane-Mimetic Environments: Molecular Basis for Neurotensin Receptor Recognition‡

Jérome Coutant,[§,||,⊥] Patrick A. Curmi,[||,⊥] Flavio Toma,[||] and Jean-Pierre Monti*[,§]

Laboratoire de Physique et Biophysique GESVAB EA 3675, Institut des Sciences de la Vigne et du Vin, Université de Bordeaux 2, 146 rue Léo Saignat, 33076 Bordeaux Cedex, France, Laboratoire Structure et Reconnaissance des Biomolécules EA 3637, Université Evry-Val d'Essonne, bâtiment Maupertuis, rue du père Jarlan 91025 Evry, France

Received December 14, 2006; Revised Manuscript Received March 3, 2007

ABSTRACT: Neurotensin (NT) is a 13-residue neuropeptide that exerts multiple biological functions in the central and peripheral nervous system. Little is known about the structure of this neuropeptide, and what is known only concerns its C-terminal part. We determined here for the first time the structure of the full-length NT in membrane-mimicking environments by means of classical proton−proton distance constraints derived from solution-state NMR spectroscopy. NT was found to have a structure at both its N and C termini, whereas the central region of NT remains highly flexible. In TFE and HFIP solutions, the NT C-terminus presents an extended slightly incurved structure, whereas in DPC it has a β turn. The N-terminal region of NT possesses great adaptability and accessibility to the microenvironment in the three media studied. Altogether, our work demonstrates a structure of NT fully compatible with its NTR-bound state.

Neurotensin (NT)[1] is a 13-residue neuropeptide, pyroGlu[1]-Leu[2]-Tyr[3]-Glu[4]-Asn[5]-Lys[6]-Pro[7]-Arg[8]-Arg[9]-Pro[10]-Tyr[11]-Ile[12]-Leu[13], which exerts multiple biological functions such as neuroleptic-like effects, an influence on thermal regulation, reduction of locomotor activity and potentiation of alcohol in the central nervous system, and neuromodulation of the vascular and endocrine systems in the peripheral nervous system (*1*).

The activities of NT are related to its binding with various affinities to different receptors (NTRs) belonging either to the superfamily of the G-protein-coupled receptors (GPCRs) (NTR1 and 2) or to the family of sorting receptors (NTR3) (*2*). Various experiments using NTR antagonists, antisense inhibition of NTRs in the brain, or knockout mice indicate that most of the activity of NT results from its interaction with NTR1 (*3*−*5*). Interestingly, it has long been known that the six amino-acid C-terminal peptide fragment of neurotensin, NT(8−13), possesses all of the sequence requirements to bind with subnanomolar affinity to NTR1, as observed with the full-length peptide (*6*, *7*). The functional role of the N-terminal region of NT remains to this date unclear. On the receptor side, mapping of the NT binding site indicates that the transmembrane domains 6 (TM6), 4 (TM4), and the third extracellular loop E3 seem to play a crucial role in NT recognition (*8*−*10*).

Despite its clinical importance, very little is known regarding the structure of NT in interaction with NTRs. Progress in this field would provide insight into the function of NT and help in understanding the specificity of its binding to various receptors. Furthermore, such information is important in order to accelerate the development of novel molecules with great putative pharmacological interest.

Various NMR methods can be used to address this question (*11*). However, unlike many other peptide hormones, few studies have examined the structure of NT using NMR. A first study showed that NT behaved as a flexible random coil in aqueous solution (*12*). Another study using SDS micelles investigated the structure of NT in environments that mimic the membrane; however, the binding of three cationic C-terminal residues of NT to the anionic sulfate head groups of micelles precluded any structure determination because of excessive line broadening on the ^{1}H NMR spectra (*13*). More recently, Pang et al., using homology modeling of the C-terminal part of NT (NT 8−13) and the E3 loop, in conjunction with experimental data, proposed that NT adopts a compact conformation when bound to NTR with a proline type I turn in its Arg[9]-Ile[12]region (*14*). This was in contradiction with the model proposed by Barroso et al., who suggested that the NT(8−13)-bound peptide adopts a rather linear conformation (*10*), using a combination of NTR1 mutagenesis, pharmacology, and molecular modeling with frog rhodopsin as an NTR1 template.

Finally, two studies used solid-state NMR-MAS (*15*) to investigate the interaction of the NT fragment NT(8−13)

‡ NMR assignments and atomic coordinates for the converged structures have been deposited with the BioMagResBank (entry 15145) and the Protein Data Bank (entries 2OYV and 2OYW) respectively.

* To whom correspondence should be addressed. Tel: 33-5-5757-1792. Fax: 33-5-5757-4563. E-mail: jean-pierre.monti@physique.u-bordeaux2.fr.

§ Université de Bordeaux 2.

|| Université Evry-Val d'Essonne.

⊥ J. Coutant and P.A. Curmi contributed equally to this work.

[1] Abbreviations: CSI, chemical shift index; DPC, dodecylphosphocholine; E3, third extracellular loop of NTR; HFIP, hexafluoroisopropanol; NMR, nuclear magnetic resonance; 2D-NMR, two-dimensional NMR; NMR-MAS, NMR-magic angle spinning; NOE, nuclear Overhauser effect; NOESY, nuclear Overhauser spectroscopy; NT, neurotensin; NTR, neurotensin receptor; rmsd, root mean square deviation; SDS, sodium dodecyl sulfate; TFE, trifluoroethanol; TM, transmembrane domain of NTR; TOCSY, total correlated spectroscopy.

10.1021/bi602567p CCC: $37.00
Published on Web 04/19/2007

with its receptor. Williamson et al. showed significant modifications in ^{13}C chemical shifts of NT(8−13) upon binding to the receptor, which pointed to an important role of the NT C-terminus and the Tyr^{11} side chain for interaction with NTR, but they did not propose any structure (*16*). Luca et al., using a ^{13}C chemical shift index for NT(8−13) upon receptor binding, suggested that NT undergoes a linear rearrangement to adopt a β-strand conformation (*17*).

Altogether, data are lacking on the structure of the full-length NT in the membrane environment or bound to its receptor, thus underlining the need for additional investigations to better understand the structure of NT bound to its receptor.

In the present work, we studied the conformation of full-length NT using proton NMR in solution and molecular modeling in three structure-promoting media: trifluoroethanol (TFE), hexafluoroisopropanol (HFIP), and dodecylphosphocholine (DPC). These solvents are known to favor the stabilization of preferred conformations in peptides and have been widely used to examine peptide conformation in such membrane-mimetic environments (*18*, *19*). In particular, DPC micelles mimic the membrane environment by forming spherical aggregates where the polar headgroups are located on the surface and the hydrophobic tail in the core. The micelles are appropriate for high-resolution liquid-state NMR studies because they have a short rotational correlation time due to their small size (*11*). Furthermore, the peptide structure bound to DPC micelles could be quite close to that bound to unilamellar vesicles, which more closely resemble the biological membrane. For Rozek et al., this could be because of a less spherical shape with an axial ration of 1:6 and thus a curvature close to that of a liposome (*20*). In the three media tested, the N- and C-terminal parts of NT presented a partial structure, whereas a high degree of flexibility remained in the intermediate part. This may be critical for modulating the pluripotency of NT.

MATERIALS AND METHODS

Materials. Neurotensin was purchased from Bachem (4006469) and was used without any further purification. Deuterated TFE-d_3, HFIP-d_2, and DPC-d_{38} were purchased from Eurisotop (Saint Aubin, France).

The NMR studies of NT conformation in TFE and HFIP were carried out with samples containing 1 mg of peptide dissolved in either of the following solvent mixtures: TFE or HFIP 80% and H_2O 20%. To prepare samples in micelles, 1 mg of peptide was dissolved with 30 mg of DPC in 120 μL of a H_2O/D_2O (12:1) mixture (final peptide concentration ~5 mM). The pH of the solution was 6.4. In these experimental conditions, the DPC concentration was higher than the critical micelle concentration and ensured a molar micelle/peptide ratio greater than 1:1, thus minimizing the peptide−peptide interaction at the micelle surface (*21*, *22*).

Spectroscopy Experiments. All of the ^1H NMR experiments were performed on a Bruker Avance 600 MHz NMR spectrometer equipped with a cryoprobe, and the spectra were recorded with 1.7 mm NMR tubes. Data were processed using XWINNMR software (Bruker). Sodium [3-methylsilyl 2,2′,3,3′-$^2H_4$] propionate (TSP-d_4) served as an internal reference for proton chemical shifts.

NT spectra in HFIP/H_2O (80:20) and in TFE/H_2O (80:20) were collected at 293 K and at 283 K in DPC micelles. For sequence-specific assignments, 2D TOCSY (*23*) and NOESY (*24*) spectra were used. The TOCSY experiments were performed with the DIPSI-2 sequence (*25*) with mixing times of 30, 50, and 70 ms in HFIP solution, and 75 ms in TFE solution and in DPC micelles. The NOESY experiments were acquired with a mixing time of respectively 100, 200, and 300 ms in HFIP, 200 and 300 ms in TFE, and in DPC micelles. All of the 2D experiments in TFE (80%) and HFIP (80%) were carried out with 2048 data points × 512 increments and a spectral width of 6614 Hz in both dimensions, 32 scans for NOESY, and 64 scans for TOCSY experiments. For neurotensin in DPC micelles, 2D experiments were carried out with 2048 data points × 512 increments × 144 scans and a spectral width of 7184 Hz in both dimensions. Water suppression was accomplished by presaturation during the relaxation delay or with a WATERGATE sequence (*26*). Temperature coefficients ($\Delta\delta/\Delta T$) were obtained with 1D spectra recorded at 283, 288, 293, 298, 303, and 308 K.

Molecular Modeling. Molecular modeling was conducted with the Accelrys software package. Simulated annealing and energy minimization were done with Discover and NMR-Refine using the consistent-valence force field (cvff) model (*27*). Interproton distances were obtained from NOESY cross peaks by integrating intensities at 300 ms mixing time and calibrating the intensities using the NOEs between the β-methylene protons of prolines (*28*). The NOE-distance constraints between two protons were estimated using a relation of the Braun model for short flexible peptides (*29*). To take spin diffusion and internal motion into account, distance constraints were classified into four categories of upper-distance limits rather than as strict constraints. Cross peaks were divided into strong, medium, weak, and very weak classes, corresponding to upper limits of 2.7, 3.3, 5.0, and 6.0 Å, respectively (*30*). Pseudoatoms were used for nonstereospecifically assigned protons, and the limits were adjusted using standard pseudoatom corrections (*31*).

Structure Calculations. Simulation annealing calculations involved 15 separate phases. The first phase involved 100 steps of randomization and minimization of the starting structure into the steepest-descent algorithm. The second phase involved additional minimization into 500 iterations of the conjugate gradient algorithm. Dynamic phases 3−5 involved simulated annealing for 30, 10, and 10 ps, respectively, at 1000 K. Meanwhile, the force constants were increased stepwise up to their full values. Phases 6−10 involved cooling of the molecule from 1000 to 300 K over 2 ps. Phases 11 and 12 involved minimization using 100 steps of the steepest-descent algorithm followed by 500 iterations of the conjugate gradient. Then, minimization phases 13 and 14, with a distance-dependent dielectric constant to mimic the solvent effect, involved 100 steps of a steepest descent followed by 1500 iterations of a conjugate gradient. Finally, the last phase involved 1500 steps of a steepest-descent algorithm with the distance-dependent dielectric constant but without the NMR constraints in order to improve the molecular relaxation.

One hundred structures of low total energy were calculated using the experimental distances determined from NOE spectra. From these, we discarded the structures with (i) violations of the distance restraint above 0.5 Å, (ii) 2 or more violations per molecule, and (iii) backbone dihedral angles

Table 1: NT Chemical Shifts of the Assigned ^{1}H NMR Resonances in HFIP/H_2O (80/20), TFE/H_2O (80/20) (in Italics), and DPC Micelles (in Bold)

	NH	Hα	Hβ	others			
pGlu[1]	7.52	4.27	2.56/1.98	Hγ 2.42/2.01			
	7.73	*4.28*	*2.54/1.95*	*2.40/1.98*			
	-	**4.35**	**2.47/1.90**	**2.37**			
Leu[2]	7.39	4.30	1.61	Hγ 1.62; Hδ 0.93/0.87			
	7.76	*4.26*	*1.61*	*1.52*		*0.94/0.88*	
	8.61	**4.23**	**1.59/1.46**	**1.54**		**0.91/0.85**	
Tyr[3]	7.44	4.46	3.06/3.02	Hδ 7.08; Hϵ 6.86			
	7.79	*4.52*	*3.08/3.00*	*7.11*		*6.86*	
	8.22	**4.56**	**3.03/2.93**	**7.06**		**6.80**	
Glu[4]	8.73	4.14	2.07/1.97	Hγ 2.45/2.32			
	8.49	*4.23*	*2.07/1.96*	*2.33/2.30*			
	8.43	**4.21**	**1.97/1.86**	**2.17**			
Asn[5]	7.81	4.76	2.92/2.81	NHδ 6.97/6.25			
	8.11	*4.75*	*2.84*	*7.36/6.56*			
	8.57	**4.65**	**2.79/2.68**	**7.73/7.04**			
Lys[6]	7.59	4.70	1.92/1.80	Hγ 1.53; Hδ 1.73; Hϵ 3.05			
	7.77	*4.69*	*1.87/1.79*	*1.51*	*1.73*		*3.03*
	8.29	**4.57**	**1.79**	**1.42**	**1.67**		**2.96**
Pro[7]		4.40	2.30/1.95	Hγ 2.12/2.04; Hδ 3.79/3.62			
		4.44	*2.30/1.93*	*2.09/2.03*		*3.81/3.63*	
		4.40	**2.28/1.84**	**1.97**		**3.78/3.59**	
Arg[8]	7.45	4.42	1.93/1.78	Hγ 1.71; Hδ 3.19; NHϵ 6.93			
	7.98	*4.43*	*1.90/1.78*	*1.71*	*3.21*		*7.25*
	8.61	**4.28**	**1.79/1.76**	**1.62**	**3.17**		**7.45**
Arg[9]	7.52	4.69	1.85/1.69	Hγ 1.63; Hδ 3.20/3.13; NHϵ 6.87			
	7.94	*4.68*	*1.80*	*1.67/1.65*	*3.22/3.17*		*7.13*
	8.52	**4.53**	**1.79/1.76**	**1.68/1.63**	**3.17**		**7.45**
Pro[10]		4.38	2.24/1.93	Hγ 2.04; Hδ 3.75/3.59			
		4.41	*2.20/1.90*	*2.01*		*3.75/3.59*	
		4.39	**2.21/1.77**	**1.95/1.94**		**3.77/3.57**	
Tyr[11]	7.08	4.57	3.09	Hδ 7.12; Hϵ 6.87			
	7.45	*4.59*	*3.10/3.07*	*7.12*		*6.86*	
	8.33	**4.50**	**3.02/2.97**	**7.10**		**6.80**	
Ile[12]	6.97	4.15	1.83	Hγ (CH_2) 1.42/1.04; Hγ(CH_3) 0.91; Hδ 0.89			
	7.45	*4.19*	*1.88*	*1.47/1.10*	*0.94*		*0.90*
	8.07	**4.08**	**1.93**	**1.44/1.10**	**0.89**		**0.85**
Leu[13]	6.95	4.33	1.65	Hγ 1.65; Hδ 0.97/0.94			
	7.31	*4.31*	*1.64*	*1.64*		*0.95*	
	7.87	**4.16**	**1.60**	**1.60**		**0.93/0.90**	

out of the peptide range in the Ramachandran plot. Structural statistics for the converged structures were then evaluated in terms of root mean square deviations (rmsd). Finally, the validity of structures was controlled by Procheck analysis (*32*).

RESULTS

The complete sequence-specific proton assignment of the NT protons was carried out using the standard technique developed by Wüthrich (*31*) and the NMR assignment and integration software Sparky (*33*) (Table 1).

The ^{1}H NMR spectra did not reveal the detectable presence of various conformers arising from the cis/trans isomerization of the two proline residues at positions 7 and 10. Both prolines were found in the trans configuration as determined from the observation in the NOESY spectra of the strong $H_{\alpha\delta}(i, i + 1)$ NOE cross peaks between each proline residue and the preceding amino acid. For all of the studies, the temperature coefficient values (< -3ppb/K) for amide protons showed the absence of intramolecular hydrogen bonds (*34*).

In the three solvent systems studied, the NOESY spectra showed a fairly large number of short- and medium-range NOEs restricted mainly to residues in the N- and C-terminal regions, indicating partial conformational stabilization in these parts of the peptide (Table 2). Noticeably, NOEs typical of α-helices were observed in none of the three solvents (*31*), in agreement with secondary structure prediction (*35*) and despite the fact that these media are α-helix stabilizers. By contrast, characteristic cross peaks of a type I turn were observed in DPC micelles over residues Pro[10]-Leu[13], that are, $d_{NN}(i, i + 1)$, $d_{NN}(i, i + 2)$, $d_{\alpha N}(i, i + 1)$, $d_{\alpha N}(i, i + 2)$, and $d_{\alpha N}(i, i + 3)$ (*31*) (Figure 1). However, the chemical shift index (CSI) values of Hα indicated that NT did not present a clearly defined secondary structure (*36*). Differences in CSIs of amide protons between alcohol and micelles were, on the contrary, striking (Figure 2) and might reflect different solvent exposure of amides in the three media.

Structure calculations provided families of 14, 15, and 14 structures in, respectively, HFIP, TFE, and DPC micelles (Figure 3). Superimposition of the backbone atoms showed that the structure of the N-terminal part (residues 2−5) was stabilized in the three media (Table 2). In TFE and DPC, this region presented an extended structure over Leu[2]-Asn[5] with an rmsd value equal to 0.59 and 0.71 Å, respectively, whereas it had a bent structure in HFIP with rmsd = 0.42 Å (Figure 3A). In the C-terminal region, the sequence Arg[8]-Ile[12] presented in both alcohols an extended structure, slightly

Table 2: NMR-Derived Restraints and Structural Statistic for the Final Lowest Energy Structures of Neurotensin

	HFIP 14 structures	TFE 15 structures	DPC 14 structures
distance restraints			
intraresidue NOEs	97	91	106
sequential NOEs	61	59	71
medium range NOEs[a]	15	14	27
total	173	164	204
rmsd analysis (Å)			
L2-I12 backbone	1.71	3.11	1.89
L2-N5 backbone	0.42	0.59	0.71
R8-L12 backbone	0.47	0.58	0.36
NOE violations (Å)			
total violations ≥ 0.3	4	5	2
average (viol. ≥ 0.3)	0.35 ± 0.04	0.37 ± 0.06	0.43 ± 0.01
total violations ≥ 0.2	5	2	8
total violations ≥ 0.1	18	13	20
average energy (kcal·mol^{-1})			
bond	44 ± 1	45 ± 1	45 ± 1
theta	62 ± 2	61 ± 2	60 ± 2
phi	18 ± 2	18 ± 2	18 ± 2
out of plane	0.2 ± 0.1	0.2 ± 0.1	0.2 ± 0.1
nonbonded	117 ± 3	119 ± 3	121 ± 2
coulomb	−37 ± 11	−44 ± 19	−25 ± 9
total	204 ± 11	199 ± 17	219 ± 9
rmsd from idealized geometry[b]			
bonds (Å)	0.013	0.013	0.013
angles (°)	2.5	1.6	2.4
Ramachandran regions (Procheck-NMR, %)			
most favored	69.8	81.5	96.8
additionally allowed	30.2	18.5	3.2
generously allowed	0	0	0
disallowed	0	0	0

[a] (i, i + 2) for TFE; (i, i + 2; i, i + 3; i, i + 4) for HFIP; (i, i + 2; i, i + 3) for DPC. [b] Reference bonds: NC, CO, C_AC, C_AC_B, NC_A and reference angles: CNC_A, C_ACN, C_ACO, C_BC_AC, NC_AC, NC_AC_B, OCN.

curved in HFIP and in TFE, with rmsd values equal to 0.47 and 0.58 Å, respectively. In DPC micelles, a bent structure close to a type I turn (*37*) was observed over the Pro[10]-Leu[13] region that followed the Arg[8]-Arg[9] sequence in extended conformation (rmsd = 0.36 Å) (Figure 3B).

Comparison of the mean structures in both alcohol solvents showed a superimposition of the backbone atoms with an rmsd value equal to 0.71 Å for the Arg[8]-Ile[12] region, with a similar spatial orientation of the side chains (Figure 4). The intermediate part, Lys[6]-Pro[7], is found to be flexible owing to the rather high rmsd values (1.71, 3.11, and 1.89 Å) when we tried to superimpose the Leu[2]-Ile[12] structures (Table 2). This flexibility was in agreement with the lack of NOE cross peaks in this central part and indicated that the conformational stabilization at both termini (sequences 2−5 and 8−12) occurred independently with no long-range interaction between these two regions.

DISCUSSION

NT is an endogenous peptide neurotransmitter that is widely distributed in the nervous system and influences various central and peripheral functions in mammals. NT is widely thought to exert these activities mainly through interaction with two G-protein coupled receptors, NTR1 and NTR2. To date, little is known at the molecular level as to how full-length NT interacts with its main receptor, NTR1.

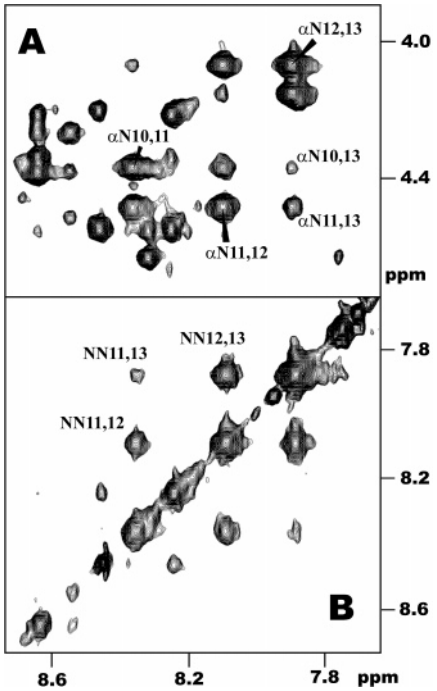

FIGURE 1: Selected region of a 600 MHz NOESY spectrum (mixing time 300 ms) of NT in DPC micelles. Cross-peak characteristics of the type I turn were annotated. Alpha/amide proton region (A) and amide proton region (B).

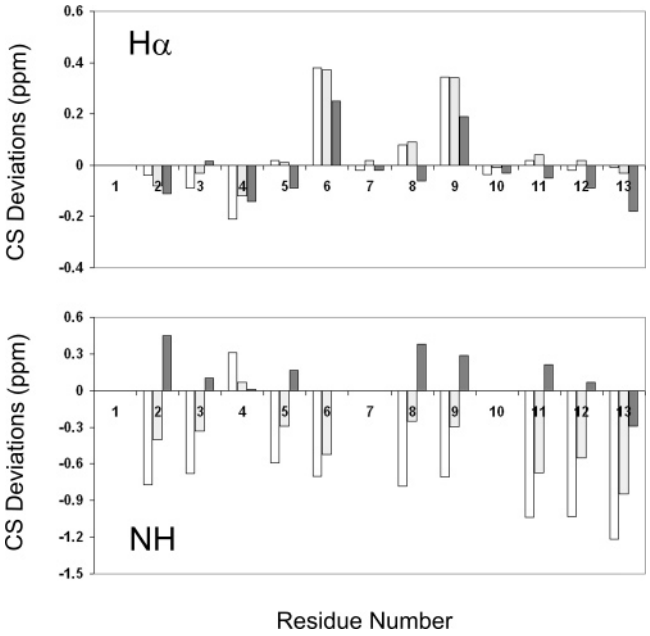

FIGURE 2: Chemical shift deviations of the Hα and amide proton resonances from random coil for NT. White and light-gray bars in HFIP and TFE solutions, respectively, dark-gray bars in DPC micelles.

The only available data are conflicting and concern the bound conformation of the C-terminal NT(8−13) peptide fragment.

Owing to the broad-range in vivo effects of NT, and because the N-terminal part of NT may influence the overall NT-bound structure and specificity of its interaction with different receptors, we investigated the solution structure of the full-length NT by means of 2D-NMR spectroscopy in three media able to mimic the membrane environment (two alcohol solvents and DPC micelles). In these media, NT was found to present a global organization with both the N and

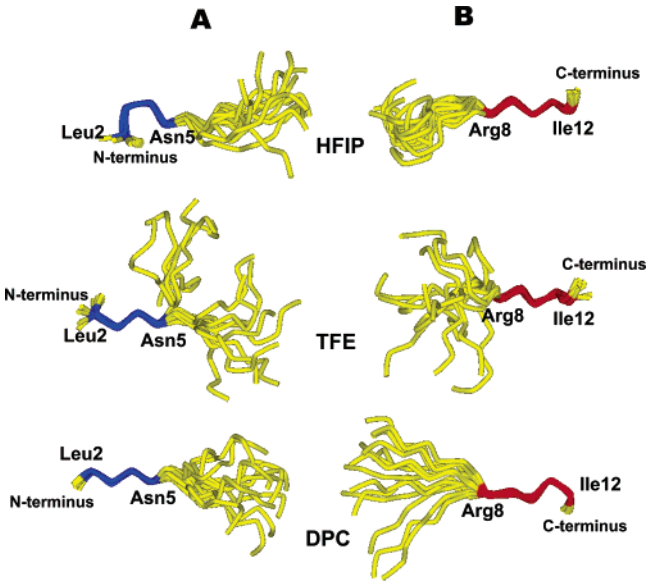

FIGURE 3: Conformations of NT in HFIP/H_2O (80%/20%), TFE/H_2O (80%/20%), solvents, and DPC micelles. The molecules were superimposed (in blue and in red) for minimum rmsd on the N-terminal region Leu^2-Asn^5 (A) and the C-terminal region Arg^8-Ile^{12}, and (B) only the backbone is represented for clarity.

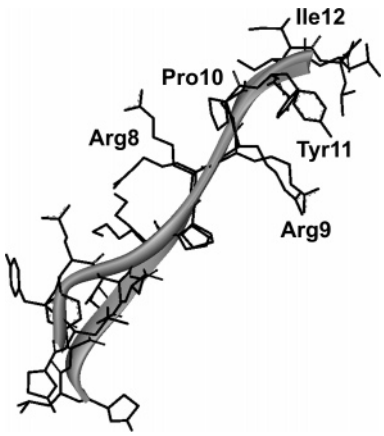

FIGURE 4: Superimposition of NT structure in both alcohol solvents. The molecules were superimposed for minimum rmsd on the C-terminal region Arg^8-Ile^{12}. The ribbons represent the NT backbone.

C termini structured, whereas a high degree of flexibility remained in its central part.

Structure of the C-Terminal Region of Neurotensin. Previous structure investigations of NT essentially concerned the C-terminal hexapeptide (Arg^8-Leu^{13}) because it was shown that this region was sufficient for receptor binding and function (*6*, *7*). Structural information regarding this region has thus been reported in three papers with proposals to account for the putative NT-/NTR-bound conformation (*10*, *14*, *17*). Two studies were conducted in the absence of experimental structural data and led to two opposite conclusions. The first proposed a compact bent conformation, which was based on de novo tertiary predictions of the structure of the NTR putative NT binding site coupled with receptor and ligand mutagenesis experiments (*14*). The second study concluded that this region adopted a linear structure. These results were derived from a model of NTR1 constructed with rhodopsin as a template, combined with mutagenesis and structure−activity relationship experiments (*10*). A recent

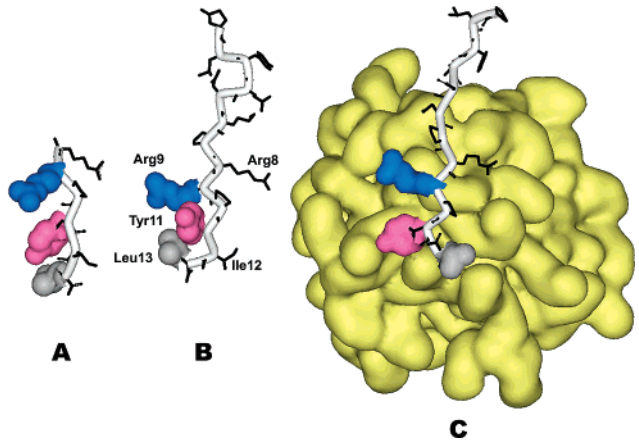

FIGURE 5: Theoretical conformation of NT in β-strand (A). Closest structure to the mean structure for NT in HFIP/H_2O (80%/20%) solvent, (B) and in DPC micelles (graphically included) (C). Side chains of Arg^9 (blue), Tyr^{11}(violet), and Leu^{13} (gray) are shown with their van der Waals surface.

study indicated that the NT(8−13) fragment bound to NTR1 presented a β-strand conformation based on ^{13}C chemical shift index analyses of the bound peptide by HR-MAS NMR and uniformly ^{13}C and ^{15}N labeled NT(8−13) in the presence of functional NTR1 reconstituted into lipid vesicles (*17*).

In this work, we show that in two different alcohol solvents (TFE and HFIP), full-length NT had, for the same C-terminal residues, an extended though slightly bent structure (Figures 3 and 4) that is very similar to the one found in the solid state for the NT(8−13) bound to the receptor. In a β-strand conformation, as proposed by Luca et al. (*17*), the side chains of three functionally important residues (Arg^9, Tyr^{11}, and Leu^{13}) of NT (*9*, *10*, *14*) are on the same side of the backbone (Figure 5A). In the solution structures (TFE and HFIP) of this work, the same key residues are also located on a β-strand, and their side chains are oriented in space by the same side of the extended backbone as in the complex (Figure 5A,B). Thus, the conformations observed in both alcohols are likely to be close to the active structure of NT bound to NTR1. In fact, our structure is close to that proposed by Luca et al. (*17*) except for the Pro^{10} (Φ, Ψ) values, which differ notably from those we found in solution (Table 3). This difference might be due to the different methods used: Luca and co-workers deduced the (Φ, Ψ) values from Cα and Cβ chemical shifts using TALOS, whereas our values were derived from an exhaustive set of NOE distance constraints. More particularly, however, a Φ value of ca. −147 does not seem realistic for a proline residue even under the constraints associated to receptor binding and is not in the range of values found for proline residues in high-resolution crystal structures of proteins (Φ Pro average value $= -66 \pm 10$ in 46 high-resolution crystal structures of proteins) (*38*). Importantly, the (Φ, Ψ) dihedral angle values of Pro^{10} in this study, and more specifically the Φ value, are in agreement with the allowed regions of proline residues shown in Procheck (*32*). Finally, our results validate the model of Barroso et al. (*10*).

Though structure elucidation in the absence of the receptor may appear at first glance to provide only limited insight into the bioactive conformation, there is emerging evidence because of the work of Schwyzer (*39*) and it is in agreement with the two-step ligand transportation theory (*40*) that

Table 3: Comparison of Φ, Ψ Dihedral Angles

	Arg9		Pro10		Tyr11		Ile12	
	Φ	ψ	Φ	ψ	Φ	ψ	Φ	ψ
theoretical β-strand[a]	−140	145	−68	157	−154	162	−152	151
this work NT in HFIP	−108 ± 11	115 ± 8	−76 ± 3	86 ± 11	−145 ± 8	125 ± 7	−97 ± 7	98 ± 4
ref 17[b]	−134 ± 31	136 ± 25	−147 ± 16	146 ± 15	−121 ± 22	131 ± 19	−114 ± 8	134 ± 24

[a] NT(8−13) was constructed in β-strand and minimized by steepest-descent algorithm with a distance-dependent dielectric constant to mimic the solvent effect. [b] Dihedral angles (φ, ψ) were obtained from an analysis using TALOS.

peptide/membrane interactions are mandatory for receptor recognition (*41*, *42*). Accordingly, bioactive peptides are thought to encounter and bind first to the membrane in a nonspecific manner, then to migrate and bind specifically to their cognate receptors by 2D diffusion on the membrane surface. It thus appears that the membrane may assist or prepare binding to the receptor by locking the peptide into a bioactive shape and that this two-step binding sequence could be kinetically more advantageous than a single-step binding scheme. Thus, NT structure was also studied in DPC micelles because this solvent closely mimics the biological membrane and is compatible with high-resolution NMR studies (*11*). A bent structure close to a type I turn was observed in the C terminus, from Pro^{10} to Leu^{13}, with Φ and Ψ values of -76 ± 5 and $-35 \pm 8°$ for Tyr^{11} and -71 ± 6 and $-18 \pm 7°$ for Ile^{12}. This folded conformation in DPC micelles was different from the extended structure found in TFE and HFIP, suggesting that the hydrophobic side-chains of the turn established interactions with the micelles. In the case of NT(8−13) and assuming that the two-step ligand transportation theory is valid, the conformational changes needed to pass from the bound-micelle molecule (turn) to the bound-receptor peptide (extended) require modifications in the main chain torsional angles of only two residues, Tyr^{11} and Ile^{12}. Thus, the energy cost to change to the bound-receptor conformation could be compensated by the energy benefit that could occur from intermolecular contacts in the receptor (Figure 5). This hypothesis agrees with a recent study where the conformation of pituitary adenylate cyclase polypeptide (PACAP) was determined, bound to its specific receptor and to DPC micelles (*42*). The conformational changes for the bioactive N-terminal region (residues 1−7) needed to pass from the bound-micelle molecule (N-terminal disordered 1−4 and α-helix 5−7) to the bound-receptor peptide (N-terminal extended segment 1−3 and β-coil 4−7) require modifications in the main-chain torsional angles of PACAP residues 4, 6, and 7. Thus, our explanation for the NT conformational rearrangement is in agreement with this study.

Structure of the N-Terminal Region of Neurotensin. This study is the first to investigate the structure of full-length NT. Whereas previous studies focused on the structure of the C-terminal NT(8−13) fragment that binds with high affinity to the receptor (*10*, *14*, *17*), nothing is known of the structure of the N-terminal part of NT (residues 1−7). This part may, however, play a role in the overall structure, modulate the interactions of NT with its partners, influence NT receptor specificity, or be directly involved in some biological effects (*43*). In fact, Pang et al. showed a significant modification of binding-constant value when they compared NT(8−13) and full-length NT (*14*). The structure of NT(2−5) was found to be similar in TFE solvent and DPC micelles showing an extended conformation, whereas it presented a turn in HFIP solution. These results suggest (i) a great adaptability of the N-terminal region to the environment because two different conformations with different spatial arrangements of side chains were obtained in both alcohol solvents with relatively close physicochemical properties and (ii) a great accessibility because the finding of similar structures in TFE and DPC micelles indicated that this region did not seem to participate in interactions with micelles and was thus accessible to the solvent (Figure 2, amide protons). Moreover, the weaker stabilization of the NT(2−5) structure in DPC micelles as deduced from the rmsd value ($rmsd_{2-5} = 0.71$ Å) as compared to that in both alcohol solvents ($rmsd_{2-5} = 0.42$ Å in HFIP and 0.59 Å in TFE) is in favor of this hypothesis. Altogether, the adaptability and the solvent accessibility of the N terminus of neurotensin are associated with the high degree of flexibility observed between the N- and C-terminal parts of NT. Such a flexible linker may allow the N-terminal part to either interact with different partners or participate in receptor specificity.

Recently, Heise et al. developed an argument against the idea of a conformational stabilization of NT in structure-promoting solvents (*44*). This argument does not seem to hold because we report here experimental evidence of the conformational stabilization of the two terminal regions of full-length NT in different solvent systems. The different conclusions in these two studies might be partly explained by the different approaches used. Heise et al. mainly used a theoretical method based on molecular dynamic simulations and Cα and Cβ chemical shifts translated into conformational parameters, whereas we used the classical solution-state NMR with proton−proton NOEs as structural data and simulated annealing structure calculations. However, definite solution structures for a peptide such as NT have to be considered as the average of structures in fast conformational exchange rather than preferred unique conformations (*11*). Clearly, in the solvents used here, the NT molecules appear to be mostly distributed in a restricted number of structural populations with defined structures in the C- or N-terminal regions. Interestingly, the average C-terminal structure of NT in both alcohols is close to the one observed for the receptor-bound C-terminal fragment (*17*) and can be therefore considered related to the bioactive, receptor-bound structure.

In conclusion, we present for the first time a structure of full-length NT compatible with its receptor-bound state obtained by the standard approach using proton−proton distance constraints derived from solution NMR and molecular modeling. Our results provide a structural model that will contribute to the fundamental knowledge of the NT interaction with its receptors and will provide insights into ligand/receptor recognition in the superfamily of the G-

protein-coupled receptors. These data may also be of practical interest for further pharmacological developments of agonist and antagonist molecules that could target different NT receptors.

ACKNOWLEDGMENT

J.P.M. and J.C. thank the Conseil Régional d'Aquitaine and the Fondation Singer-Polignac for financial support. The Conseil Régional d'Ile de France, the Conseil Général de l'Essonne, the Genopole, the CEA/DSV, and the AFM are gratefully acknowledged for the NMR equipment of the LSRB. P. A. C. is the recipient of an ATIGE grant from Genopole EVRY. We are also grateful to Dr. Ray Cooke for editing the manuscript. In memory of Professor G. A. Gacel.

REFERENCES

1. Vincent, J. P., Mazella, J., and Kitabgi, P. (1999) Neurotensin and neurotensin receptors, *Trends Pharmacol. Sci. 20*, 302−309.
2. Kitabgi, P. (2002) Targeting neurotensin receptors with agonists and antagonists for therapeutic purposes, *Curr. Opin. Drug. Discovery Dev. 5*, 764−776.
3. Dubuc, I., Sarret, P., Labbe-Jullie, C., Botto, J. M., Honore, E., Bourdel, E., Martinez, J., Costentin, J., Vincent, J. P., Kitabgi, P., and Mazella, J. (1999) Identification of the receptor subtype involved in the analgesic effect of neurotensin, *J. Neurosci. 19*, 503−510.
4. Pettibone, D. J., Hess, J. F., Hey, P. J., Jacobson, M. A., Leviten, M., Lis, E. V., Mallorga, P. J., Pascarella, D. M., Snyder, M. A., Williams, J. B., and Zeng, Z. (2002) The effects of deleting the mouse neurotensin receptor NTR1 on central and peripheral responses to neurotensin, *J. Pharmacol. Exp. Ther. 300*, 305−313.
5. Gully, D., Canton, M., Boigegrain, R., Jeanjean, F., Molimard, J. C., Poncelet, M., Gueudet, C., Heaulme, M., Leyris, R., Brouard, A., Pelaprat, D., Labbe-Julie, C., Mazella, J., Soubrie, P., Maffrand, J., Rostene, W., Kitabgi, P., and Le Fur, G. L. (1993) Biochemical and pharmacological profile of a potent and selective nonpeptide antagonist of the neurotensin receptor, *Proc. Natl. Acad. Sci. U.S.A. 90*, 65−69.
6. Kitabgi, P., Carraway, R., Van Rietschoten, J., Granier, C., Morgat, J. L., Menez, A., Leeman, S., and Freychet, P. (1977) Neurotensin: specific binding to synaptic membranes from rat brain, *Proc. Natl. Acad. Sci. U.S.A. 74*, 1846−1850.
7. Granier, C., van Rietschoten, J., Kitabgi, P., Poustis, C., and Freychet, P. (1982) Synthesis and characterization of neurotensin analogues for structure/activity relationship studies. Acetyl-neurotensin-(8−13) is the shortest analogue with full binding and pharmacological activities, *Eur. J. Biochem. 124*, 117−124.
8. Cusack, B., Groshan, K., McCormick, D. J., Pang, Y. P., Perry, R., Phung, C. T., Souder, T., and Richelson, E. (1996) Chimeric rat/human neurotensin receptors localize a region of the receptor sensitive to binding of a novel, species-specific, picomolar affinity peptide, *J. Biol. Chem. 271*, 15054−15059.
9. Richard, F., Barroso, S., Nicolas-Etheve, D., Kitabgi, P., and Labbe-Jullie, C. (2001) Impaired G protein coupling of the neurotensin receptor 1 by mutations in extracellular loop 3, *Eur. J. Pharmacol. 433*, 63−71.
10. Barroso, S., Richard, F., Nicolas-Etheve, D., Reversat, J. L., Bernassau, J. M., Kitabgi, P., and Labbe-Jullie, C. (2000) Identification of residues involved in neurotensin binding and modeling of the agonist binding site in neurotensin receptor 1, *J. Biol. Chem. 275*, 328−335.
11. Pellegrini, M., and Mierke, D. F. (1999) Structural characterization of peptide hormone/receptor interactions by NMR spectroscopy, *Biopolymers 51*, 208−220.
12. Nieto, J. L., Rico, M., Santoro, J., Herranz, J., and Bermero, F. J. (1986) Assignment and conformation of neurotensin in aqueous solution by 1H NMR, *Int. J. Peptide Protein Res. 28*, 315−323.
13. Xu, G. Y., and Deber, C. M. (1991) Conformations of neurotensin in solution and in membrane environments studied by 2-D NMR spectroscopy, *Int. J. Pept. Protein Res. 37*, 528−535.
14. Pang, Y. P., Cusack, B., Groshan, K., and Richelson, E. (1996) Proposed ligand binding site of the transmembrane receptor for neurotensin(8−13), *J. Biol. Chem. 271*, 15060−15068.
15. Luca, S., Heise, H., Lange, A., and Baldus, M. (2005) Investigation of ligand-receptor systems by high-resolution solid-state NMR: recent progress and perspectives, *Arch. Pharmacol. 338*, 217−228.
16. Williamson, P. T., Bains, S., Chung, C., Cooke, R., and Watts, A. (2002) Probing the environment of neurotensin whilst bound to the neurotensin receptor by solid state NMR, *FEBS Lett. 518*, 111−115.
17. Luca, S., White, J. F., Sohal, A. K., Filippov, D. V., van Boom, J. H., Grisshammer, R., and Baldus, M. (2003) The conformation of neurotensin bound to its G protein-coupled receptor, *Proc. Natl. Acad. Sci. U.S.A. 100*, 10706−10711.
18. Li, H., Li, F., Sun, H., and Qian, Z. M. (2003) Membrane-inserted conformation of transmembrane domain 4 of divalent-metal transporter, *Biochem. J. 372*, 757−766.
19. Fadhil, I., Schmidt, R., Walpole, C., and Carpenter, K. A. (2004) Exploring deltorphin II binding to the third extracellular loop of the delta-opioid receptor, *J. Biol. Chem. 279*, 21069−21077.
20. Rozek, A., Friedrich, C. L., and Hancock, E. W. (2000) Structure of bovine antimicrobial peptide indolicidin bound to dodecylphosphocholine and sodium dodecyl sulfate micelles, *Biochemistry 39*, 15765−15774.
21. Brown, L. R., Bosch, C., and Wüthrich, K. (1981) Location and orientation relative to the micelle surface for glucagon in mixed micelles with dodecylphosphocholine: EPR and NMR studies, *Biochim. Biophys. Acta 642*, 296−312.
22. McDonnell, P. A., and Opella, S. J. (1993) Effect of detergent concentration on multidimensional solution NMR spectra of membrane proteins in micelles, *J. Magn. Reson. B 102*, 120−125.
23. Braunschweiler, L., and Ernst, R. R. (1983) Coherence transfer by isotropic mixing: Application to proton correlation spectroscopy, *J. Magn. Reson. 53*, 521−528.
24. Kumar, A., Ernst, R. R., and Wüthrich, K. (1980) A two-dimensional nuclear Overhauser enhancement (2D NOE) experiment fort the elucidation of complete proton-proton cross-relaxation networks in biological macromolecules, *Biochem. Biophys. Res. Commun. 95*, 1−6.
25. Shaka, A. J., Lee, C. J., and Pines, A. (1988) Iterative schemes for bilinear operators; application to spin decoupling, *J. Magn. Reson. 77*, 274−293.
26. Piotto, M., Saudek, V., and Sklenar, V. (1992) Gradient-tailored excitation for single-quantum NMR spectroscopy of aqueous solutions, *J. Biomol. NMR 6*, 661−665.
27. Dauber-Osguthorpe, P., Roberts, V. A., Osguthorpe, D. J., Wolff, J., Genest, M., and Hagler, A. T. (1988) Structure and energetics of ligand binding to proteins: E. Coli dihydrofolate reductase-trimethoprim, a drug-receptor system, *Proteins: Struct., Funct., Genet. 4*, 31−47.
28. Pellegrini, M., Mammi, S., Peggion, E., and Mierke, D. F. (1997) Threonine6-bradykinin: structural characterization in the presence of micelles by nuclear magnetic resonance and distance geometry, *J. Med. Chem. 40*, 92−98.
29. Braun, W., Bösch, C., Brown, L. R., Go, N., and Wüthrich, K. (1981) Combined use of proton-proton Overhauser enhancements and a distance geometry algorithm for determination of polypeptide conformations. Application to micelle-bound glucagon, *Biochim. Biophys. Acta 667*, 377−396.
30. Constantine, K. L., Friedrichs, M. S., Detlefsen, D., Nishio, M., Tsunakawa, M., Furumai, T., Ohkuma, H., Oki, T., Hill, S., Bruccoleri, R. E., Lin, P. F., and Mueller, L. (1995) High-resolution solution structure of siamycin II: novel amphipathic character of a 21-residue peptide that inhibits HIV fusion, *J. Biomol. NMR 5*, 271−286.
31. Wüthrich, K. (1986) in *NMR of Proteins and Nucleic Acids*, (Wüthrich, K., Ed.) Wiley and Sons, New-York.
32. Laskowski, R. A., Rullmannn, J. A., MacArthur, M. W., Kaptein, R., and Thornton, J. M. (1996) AQUA and PROCHECK-NMR: programs for checking the quality of protein structures solved by NMR, *J. Biomol. NMR 8*, 477−486.
33. Goddard, T.D., and Kneller, D.G., *SPARKY 3*, University of California, San Francisco.

34. Kotovych, G., Cann, J. R., Stewart, J. M., and Yamamoto, H. (1998) NMR and CD conformational studies of bradykinin and its agonists and antagonists: application to receptor binding, *Biochem. Cell Biol. 76*, 257−266.
35. Muñoz, V., and Serrano, L. (1997) Development of the multiple sequence approximation within the Agadir model of α-helix formation. Comparison with Zimm-Bragg and Lifson-Roig formalisms, *Biopolymers 41*, 495−509.
36. Wishart, D. S., and Case, D. A. (2001) Use of chemical shifts in macromolecular structure determination, *Methods Enzymol. 338*, 3−34.
37. Chou, K. C. (2000) Prediction of tight turns and their types in proteins, *Anal. Biochem. 286*, 1−16.
38. Priestle, J. P. (2003) Improved dihedral-angle restraints for protein structure refinement, *J. Appl. Crystallogr. 36*, 34−42.
39. Schwyzer, R. (1986) Molecular mechanism of opioid receptor selection, *Biochemistry 25*, 6335−6342.
40. Adam, G., and Delbrück, M. (1968) Reduction of dimensionality in biological diffusion processes, in *Structural Chemistry and Molecular Biology* (Rich, A. and Davidson, N., Eds.), pp 198−215, W. H. Freeman, San Francisco.
41. Bader, R., Bettio, A., Beck-Sickinger, A. G., and Zerbe, O. (2001) Structure and dynamics of micelle-bound neuropeptide Y: comparison with unligated NPY and implications for receptor selection, *J. Mol. Biol. 305*, 307−329.
42. Inooka, H., Ohtaki, T., Kitahara, O., Ikegami, T., Endo, S., Kitada, C., Ogi, K., Onda, H., Fujino, M., and Shirakawa, M. (2001) Conformation of a peptide ligand bound to its G-protein coupled receptor, *Nat. Struct. Biol. 8*, 161−165.
43. Sicard, F., Contesse, V., Lefebvre, H., Ait-Ali, D., Gras, M., Cartier, D., Decker, A., Chartrel, N., Anouar, Y., Vaudry, H., and Delarue, C. (2006) The N-terminal neurotensin fragment, NT1−11, inhibits cortisol secretion by human adrenocortical cells, *J. Clin. Endocrinol. Metab. 91*, 3131−3137.
44. Heise, H., Luca, S., de Groot, B. L., Grubmüller, H., and Baldus, M. (2005) Probing conformational disorder in neurotensin by two-dimensional solid-state NMR and comparison to molecular dynamics simulations, *Biophys. J. 89*, 2113−2120.

BI602567P